CHAPTER 10

The Other End of Human–Robot Interaction

Models for Safe and Efficient Tool–Tissue Interactions

Árpád Takács, Imre J. Rudas, and Tamás Haidegger

CONTENTS

10.1 Introduction 137
10.2 Types of Tool–Tissue Interaction 139
10.3 Review of Control Aspects of Tool–Tissue Interactions 143
10.4 Haptic Feedback in Telesurgery 145
10.5 Soft Tissue Models 147
10.6 Methods for Modeling Soft Tissues 149
10.6.1 Mass–Spring–Damper Models 149
10.6.2 Data Collection Methods 153
10.6.3 Indentations Tests 154
10.6.4 The Proposed Nonlinear Mass–Spring–Damper Model 158
10.7 Results 160
10.7.1 Model Verification Methods 161
10.7.2 Model Verification Results 163
10.8 Usability of the Proposed Model 164
10.9 Discussion 165
Acknowledgment 165
References 165

10.1 INTRODUCTION

In the past few years, research activities related to robotic surgery have gained attention due to the rapid development of interventional systems, representing a fine example of Human–Robot Interaction (HRI) [1]. Along with the development of novel technologies, engineers and robotic experts are facing new challenges, as a completely new type of

interaction has appeared between humans and robots: human tissues manipulated by a robotic arm. Contrary to traditional HRI approaches, in the case of tool–tissue interaction, different types of models need to be used during the design and development processes, which can be reliably and safely used in manipulation-specific ranges of force values and tool movement. The new challenges carry unprecedented risks as well, especially during invasive interventions, remote surgeries, or automated task execution. While many surgical maneuvers have already been implemented with a degree of autonomy, most of today's robotic surgery devices are still used as teleoperation systems. This means that a human surgeon as an operator is always required to be present in the control loop. Parallel to the evolution of telesurgery, different model-based control methods have been developed and experimentally tested for enhancing transparency and increasing latency-tolerance, both in terms of long distance (space robotics, intercontinental operations) and short distance (local on-Earth scenarios) teleoperation. The effectiveness of traditional real-time control methods decreases significantly with the increase of time-delay, while time-varying latency introduces new challenges. A suitable control design can ensure high quality control signals and improved sensory feedback. This can only be achieved by suitable models for all components of the telesurgical systems, including models of the human operator, the slave robot, and the mechanism of tool-tissue interaction. Using bilateral haptic devices, and accounting for tissue dynamics, can handle issues arising from communication latency. Stability and accuracy deterioration caused by latency and other external disturbances, such as contacting hard tissues or elastic tool deformation, can also be addressed using realistic soft tissue models, their integration into model-based force control algorithms largely increases the robustness and reliability of robot-assisted interventions.

Automation in the field of medicine is already present in many forms, providing a solid background to the medical robotics domain to nurture on. Most medico-surgical processes follow specific guidelines, such as generic diagnostic and treatment plans, supporting medical decision making and practice. On this highest level of abstraction, automation is part of the surgical field as well, with pre-defined treatment plans for common diseases, and with the rapid development of computer-integrated surgery (CIS), automation is penetrating into the fundamental layers of surgical practice, addressing the current issues of HRI from the robot-patient perspective.

Probably the most important characteristic of many surgical robots is spatial accuracy—inherently determining their applicability, functionality, and safety. Precision of robotic systems can be represented by the accuracy and repeatability of the device to characterize the overall effect of the encoder's fineness, the compliance of the hardware elements (e.g., the servos), and the rigidity of the structure. Generally, the absolute positioning accuracy shows the error of the robot when reaching for a prescribed position. This expresses the mean difference between the actual pose and the pose calculated from the mathematical model of the robot. Repeatability is the standard deviation of the positioning error acquired through multiple trials to reach the same joint values. Repeatability is typically smaller for manipulators than accuracy, and both numbers can largely depend on speed, payload, and range of motion.

Followed by the discussion of the importance of tool–tissue interaction modeling, control aspects, and haptic feedback in telesurgery, this chapter presents a methodology for soft tissue modeling. The motivation is to present tool–tissue interaction scenarios, from the HRI point of view. We present a specific but generalizable use case, where the tissue deformation is uniform along the surface, verifying the proposed soft tissue model and highlighting the limitation of linear heuristic models. Then, we discuss a more complex approach, utilizing nonuniform surface deformation, estimating the force response from the previously verified model. The mechanical parameters of the soft tissue model, including stiffness and damping values of the elements, are estimated from measurement data, taken from the experiments described in the sections in detail.

10.2 TYPES OF TOOL–TISSUE INTERACTION

Tool–tissue interaction is the phenomenon when the surgical tool in some physical way interacts with the tissue to be manipulated during the intervention. Depending on the circumstances of the interaction, there are many types of manipulations that can be distinguished based on the instrument geometry, biological properties of the tissue, invasiveness of the interaction, and the mathematical modeling approach of the intervention.

When the surgical intervention is assisted by a robotic system, from the HRI point of view, some of the basic types of tool–tissue interactions are the following. In terms of invasiveness, the manipulation can be carried out using *blunt* instruments (tissue palpation for tumor detection, moving of organs for accessing the surgical area), *sharp* instruments (cutting, suturing, needle insertion), or *special* instruments (coagulation, ablation). In terms of the available feedback, the operator may receive *visual* information (endoscopic cameras, tool position mapping to pre-operative images), *haptic* feedback (direct on indirect force feedback, tactile feedback, haptic guidance), or *audio/audiovisual* feedback (forbidden region restriction, virtual fixtures, proximity information of the tool to the area of interest). Types of tool–tissue interaction can be approached from the mechanical properties and modeling of the participating mediums. We can differentiate between *soft tissue* interaction (organs, skin, muscles) and *hard tissue* interaction (primarily bones in drilling tasks or collision warning), while from the tool modeling aspect, *rigid tools* (scalpel blade), *elastic tools* (needles, MIS instruments), and *hybrid flexible tools* (snake-like tools, cable-driven manipulators). The modeling of tool/tissue deformation, reaction forces and biomechanical transitions (rupturing, chemical reactions) is a complex coupled problem, therefore, the *model complexity* also plays an important role in addressing a type of tool–tissue interaction. The most popular approaches—not restricted to the tissue models—include *continuum-mechanics based* models (complex deformations, highly nonlinear systems, FEA modeling), *heuristic* models (low degree of freedom tasks, simple manipulations, high-level behavior estimation), and *hybrid* models.

AU: Please expand acronym FEA

A comprehensive study about the existing soft tissue models used in most MIS applications and virtual surgical simulators was presented by Famaey and Sloten [2], introducing three major categories of deformation models: heuristic models, continuum-mechanics models, and hybrid models. The complexity of each model mentioned above varies on a wide scale, although it is commonly accepted that approaches based on continuum-mechanics

provide a more realistic response but requires significantly higher computational capacity. An analytical solution to the used mathematical laws generally does not exist. On the contrary, heuristic models that consist of lumped, linear mass–spring–damper elements, sometimes also called mechanical models, can be used for describing simple surgical tasks like needle insertion. The derived equations can usually be solved analytically.

While the modeling of soft tissue behavior has been the focus of research for a long time, the challenging field of gaining information about the interactions of the robot arm and the tissue has only reached popularity recently. Among the arising issues, it is important to mention the problem of force feedback, the modeling of tools, and the interaction with organs itself. A comprehensive review on current tool–tissue interaction models was carried out in [3], providing a survey on research focusing on interactions described by models, following the principles of continuum mechanics and finite element methods. The focus of interest can also be extended to models of telesurgical applications, without strict boundaries of categories, giving an overview of model properties. In [4], a simple 1 degree-of-freedom (DoF) model of a rigid master and flexible slave connection was introduced. Here, the problem of tool flexibility is addressed as one of the greatest issues in the case of tool tissue interactions, since the force sensing can only be applied at the fixed end of the tool and its deflection can only be estimated. Besides tool flexibility, the compliant parameters of the robotic arm and the tissue model are also important and are significant parts of the tool tissue interaction system. Other extensions of the model exist for rigid slave, flexible joint, and flexible master descriptions, and the complexity of the model of the whole system can be high. The great advantage of this approach is that not only the tool flexibility but the whole transparency of the system is addressed. It is important to mention, though, that no detailed tissue modeling is provided, the use of rigid specimen model indicates that this approach is rather focusing on teleoperation. Basdogan et al. [5] addressed the importance of tool–tissue interaction modeling in medical training through simulation in virtual reality, focusing on issues in haptics in minimally invasive surgery. When working with soft tissues, the elastic behavior of the tool can usually be omitted, using rigid models of surgical accessories. In their work, they introduced two new approaches to tissue modeling: the mesh-based FEA model, using modal analysis and the real-time meshless method of finite spheres. In the virtual environment, collision detection and perception of multiple tissue layers were created, accompanied with force and torque feedback to the user's hand. This feature is supported by force and position sensors mounted on the tool, which is held by the user instead of a robotic arm. The complexity of the above-mentioned methods is in connection with the required computational effort. In simple problems, the use of the method of finite spheres is suggested. Another approach to meshless methods was introduced by Bao et al., where several layers were used as the model of the soft tissue, their interaction modeled with a heuristic Kelvin model [6]. Modeling of two important viscoelastic properties, the creep and relaxation is possible with this new three-parameter viscoelastic model, improving the performance of conventional mass–spring–damper approaches. Yamamoto suggested a method for the detection of lumps in organ tissues such as the kidney, liver, and heart [7]. The importance of this work was a comprehensive comparison of seven different tissue models used in point-to-point palpation. The aim of

the tests and model validations was to create a graphical overlay system that stores data on palpation results, creating a color scale overlay on the actual tissue, processing the acquired data using several tissue models, with a single 1 DoF force sensor at the fixed end of the tool. Yamamoto et al. also created an interpolable interface with haptic feedback and augmented visual feedback and performed palpation and surface detection tasks using vision-based forbidden-region virtual fixtures [8]. The tests were carried out on manufactured artificial tissues based on existing commercially available artificial prostate, using a complex, but—based on previous measurements—accurate Hunt–Crossley model. Position, velocity, and force sensors were mounted on a slave manipulator and the visual feedback to the human user was generated with a stereo-vision system.

When dealing with viscoelastic materials interacting with tools, coupled problems arise where additional mechanical models are required to describe the system response. It is important to mention that even when the best-suited mathematical models are employed, material properties (Young-modulus, Poisson-ratio, etc.) can only be estimated. Validation of their values requires circumstantial physical experiments. When using heuristic, mechanical tissue models, the acquisition of explicit, but general material properties are omitted. Instead of using tables and possible ranges of these properties, spring and damping coefficients must be obtained from measurements even when nothing else but the tool shape is changed. In their work, Leong et al. introduced and validated a mechanical model of liver tissue and its interaction with a scalpel blade, creating a distributed model of mechanical viscoelastic elements [9]. With the serial connection of a Maxwell and a Kelvin element, they introduced the Maxwell–Kelvin viscoelastic body. The primary aim of their work was to account for the tissue surface deformation due to the extensive shape of the tool, validating with the cutting experiment where a 1 DoF force sensor was placed at the scalpel blade holder integrated with position measurement. Besides many constitutive ideas, a great number of deficiencies can be found in the model that still needs to be improved, including mathematical errors in modeling, contradictions in the measurement result evaluation, inappropriate use of Laplace transformation, and the overall pertinence of experimental results. Liu et al. introduced a method for force control for robotic-assisted surgery on a beating heart, thus applying motion compensation for the periodic motion of the organ [10]. By installing a force sensor at the end of the instrument and tracking the 3D motion of the beating heart, they compared four different models from the viewpoint of tracking performance of the desired force. Besides the conventional viscoelastic models, a fourth, fractional derivative model of viscosity was examined. One of the relevant results of this experiment was to underline the importance of the right choice of tissue model.

In the past few years, much focus has been drawn on needle insertion modeling. Due to the simplicity of the tool geometry, needle insertion problems were much discussed using Finite Element modeling. The Finite Element Method is a widely used approach for tool tissue interaction modeling, where commercially available FEA software packages are used to aid and simulate the operation area. The great many built-in mechanical models can provide incredibly accurate and realistic solutions for simulation. One of the largest drawbacks of this method is the sensitivity of computational time length with respect to the parameters used in FE simulations. These parameters are determined

solely by the user, including spatial and time resolutions, thus, many simulations need to be carried out on the same model to achieve the desired level of reliability. Goksel et al. introduced a novel technique to use real-time remeshing in the case of FEA modeling [11]. A mesh-based linear elastic model of both the needle and tissue was used, applying remeshing in order to compensate organ shift due to the invasiveness. The importance of the model is that both tool and tissue deformation were accounted for, although the motion models were the simplest possible in 3D. Continuum mechanics also provides numerous models that can be used for modeling organ and tissue deformations and kinetics.

Approaches using linear and nonlinear models of elasticity are widely used in practice. Linear models have limited usability despite the many advantages they carry (simplicity, easy-calculation, and small requirements on computational capacity) due to inhomogeneous, anisotropic, nonlinear characteristics of tissues and large relative deformations and strains. However, nonlinear models in continuum mechanics lead to moderately complex models even in simple surgical tasks. Misra et al. introduced a detailed complex mechanical model of continuum mechanics for the analytical modeling and experimental validation of needle bending at insertion into soft tissues [12]. A hyperelastic neo-Hookean rupture model was used to describe the material properties and behavior of the soft tissue simulant (gel), assuming linear elasticity in case of the needle. Experiments were carried out using different bevel-tipped needles and the needle bending curvature was validated using unfiltered camera data. The importance of the work lays in the area of needle insertion path planning.

In the area of tool–tissue interaction research, one might be interested in rapture modeling. While most of the existing mechanical models assume reversible tissue deformation, even in the case of minimal invasive surgery (MIS), tissue rupture cannot be avoided. Mahvash and Dupon developed an analytical model of tissue rapture during needle insertion, focusing on the calculation of required insertion force [13]. The great advantage of this model is that despite the complex mechanical structure, the insertion events are divided into four different models, decomposing the process into moderately complex parts. Tissue modeling was aided with a modified Kelvin model, making the parameters of the linear components dependent of the deformation rate. The analytical model validated the experiments showing that the required insertion force is inversely proportional to the insertion speed.

It is important to mention models that are not directly describing insertion and cutting problems, but are rather used for investigating interaction of cable-driven manipulators controlled by human operators, acting on soft tissues. Kosari et al. introduced an adaptive parameter estimation and model predictive control (MPC) method on cable-driven surgical manipulators, developing a 1 DoF mechanical model, concentrating on the problem of trajectory tracking [14]. Therefore, instead of the estimation of tissue reaction forces, focus was drawn to the response of the cable-driven manipulator in order to create a realistic force feedback to the human user. The moderately complex model accounts for numerous mechanical properties and solves an optimal control problem for automating tissue compression.

The proper modeling of tool–tissue interactions is a relevant topic in standardization methods. With the help of initial calculations and simulations, efficient control methods can be chosen to avoid undesired pain and injury levels. Pain and injury onset levels for static contact force and peak pressure values are deeply researched and standardized in the literature [15].

10.3 REVIEW OF CONTROL ASPECTS OF TOOL–TISSUE INTERACTIONS

The general concept of teleoperation has long been used in various fields of robotics, including manufacturing, logistics, and service robotics scenarios [16]. Today, long-distance teleoperation is an actively discussed topic in space exploration [17] and for intervention in hazardous environments [18]. Where traditional control algorithms might fail, latency-induced challenges can be addressed by novel ideas, including soft computing methods, neural control [19], supervisory control through Internet communication [20], passivity-based control [21], and various types of MPC for transparent teleoperation [22] and hybrid MPC solutions to neural network (NN)-based control methods [23].

Commercially available telesurgical systems utilize the concept of unilateral teleoperation, where the position and/or force data from the master console are transmitted to the slave system, whereas the operator only receives visual feedback from the environment through the mounted camera system. However, in bilateral teleoperation, there is a communication of force and position data in both directions of the teleoperation system. This structure allows haptic feedback to the operator, therefore, an extended virtual presence can be established in the physical surgical environment, increasing the *transparency*, which gives an answer to what level the master operator feels that the slave-side environment is being manipulated [24]. In telesurgery, the term *transparency* mostly refers to the level of match between the mechanical impedance of the manipulated environment encountered by the slave and the mechanical impedance transmitted to or felt by the operator at the master [25]. The general concept of bilateral teleoperation is shown in Figure 10.1 [26]. There is a vast literature of control architectures addressing challenges and proposing solutions to bilateral teleoperation systems, emphasizing the effect of time-delay caused by the communication latency between the master and slave sides. A large percentage of these approaches are variations of position–position teleoperation [27], position–force [28], or force–force teleoperation [29]. Other approaches include a special group of linear controllers, robust H_{inf} control, system dynamics assessment, and adaptive nonlinear controllers [30, 31, 32]. Obstacle avoidance, motion guidance, and inertia scaling also play an important role in describing the dynamics of the specific teleoperation task, where passive decomposition [33] and time-domain passivity controllers [34] can enhance the performance of actions.

Depending on the nature of the applications, the latency in communication can range between milliseconds (Internet-based teleoperation in terrestrial conditions) to several minutes (space exploration). Therefore, the magnitude of time-delay is determined by the distance between the master and slave devices and the medium of communication. It is a common view that in robotic systems, time-delay causes a trade-off between teleoperation stability and the control performance of the system. Local force feedback at the master side largely affects the performance and transparency of time-delayed teleoperation systems,

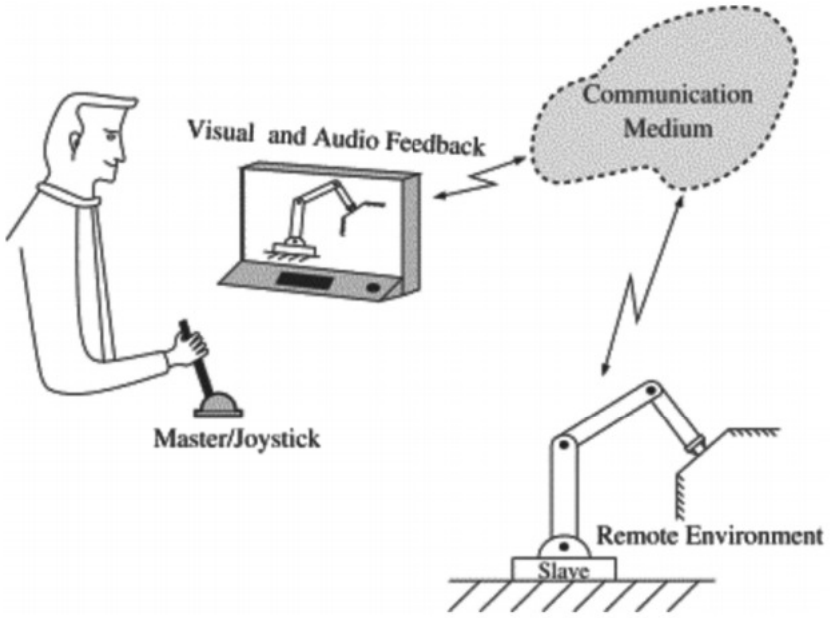

FIGURE 10.1 The concept of bilateral teleoperation by Hokayem and Spong [26].

which varies for different bilateral teleoperation architectures and the magnitude of the latency [35]. A common approach to increase the robustness of delayed teleoperation is to apply additional damping on both the master and slave side of the system, however, this often leads to a slow response of the system [36], degrading its control performance. As the transparency of the system decreases, some methods can compensate for the performance decay in bilateral teleoperation by using scattering theory [37], wave-variable control [38], or passivity control [39]. Other approaches include the telemonitoring of force feedback under low latencies [40].

In the past few decades, it has become a common view that large delays require accurate models of the operation environment based on prediction, creating a quasi-real-time simulated response to the operator [41]. One of the most successful approaches to predictive control methods utilizes the Smith predictor [42], while several approaches combine the Smith predictor with Kalman filtering for achieving better performance results [43, 44]. The linear approximation of the effect of time-delay is also a common modeling approach in teleoperation control, utilizing the state-space representation of the system based on the first-order Taylor-expansion of the system [45, 46].

In order to summarize the challenges and current possibilities in teleoperation with time-delay in the range of a few seconds, a detailed report has been published by NASA [47] in 2002. The report lists some of the most important tools and guidelines in teleoperation, highlighting the importance of predictive displays, where a realistic model of the environment is shown to the operator, which responds to the master console input in real-time. This approach has proven to be very efficient if the latency is under one second, however, it requires a reliable model of the task environment, including the slave and slave-environment interaction models [48]. Another frequently discussed issue is related to the compliance of the slave side, as it can reduce the execution time and the overall forces

acting on the environment during manipulation [49]. From the haptics point of view, force reflection in bilateral teleoperation is critical in terms of stability. In real-life applications, direct force feedback can only be applied reliably with latencies under two seconds, however, in this range, high performance in completing teleoperation tasks, in terms of stability and transparency, can only be achieved with force feedback [50]. This feedback can be achieved in numerous ways, directly or indirectly, such as using a visual feed on the force magnitude or reflection of the force of the hand of the operator that does not take part in the teleoperation. The best solution is considered to be when the interaction force is simulated and fed back to the operator based on the system model. This work gives a proposal for modeling methodology of the interaction environment during teleoperation, more precisely, the modeling of tool-tissue interaction in case of telesurgical manipulations on soft tissues, since it is a key element of HRI in surgery.

10.4 HAPTIC FEEDBACK IN TELESURGERY

In recent years, the number of MIS procedures has increased significantly. MIS allows shorter patient recovery time and the decrease of surgical trauma. However, due to the long, rigid design of MIS tools, limited vision and confined operation space, several ergonomic difficulties and technological limitations have arisen that are yet to be solved. These include the deprivation of dexterity, loss of depth perception due to the two-dimensional video image feedback, distributed hand–eye coordination and special tool manipulation, and most importantly, the loss of tactile feedback [51]. Most of these limitations were addressed and partially solved with the introduction of robot-assisted surgery and telesurgery. By using stereo visual feedback, tremor filtering and ergonomic human–machine interfaces (HMIs), the lack of force feedback limits the ability of the surgeon during organ palpation, tumor localization, and the location of other abnormalities [52].

The role of haptic feedback in telesurgery is twofold: 1) restoring tactile information is essential for assessing the surface properties of the investigated organs. This feature is generally useful for artery and lump detection, therefore, the lack of tactile feedback leads to a more difficult localization of palpable anomalies, such as kidney stones; 2) haptics may provide a realistic force feedback to the robot operator, giving information about the mechanical characteristics of the tissue. This may improve the quality of basic surgical maneuvers (grabbing, palpation, cutting), and allows collision detection, which opens new opportunities toward virtual fixtures and the design of surgical simulators [53]. Tissue characterization also requires complex perception of the operating environment, where, besides tissue stiffness (hardness), relaxation properties and other viscoelastic phenomena can be investigated and accounted for when using haptic feedback. It was also shown that for tissue characterization tasks, utilizing force feedback leads to better results than only visual feedback, while with the combination of the two, superior results can be achieved [54].

While the lack of haptic feedback is still common to modern robot-assisted MIS procedures, the solutions provided by today's commercially available telesurgical systems are still limited. Increased cost, sterilization difficulties, and the sizing limitations of force sensors at the end effector are the key limiting factors to introducing haptic feedback to these systems through direct force sensing at the tool tip. To address these issues, several

approaches were investigated for indirect force estimation, for example, accounting for joint flexibility [4], the dynamics of cable-driven manipulators [14], or force estimation through soft tissue modeling [55].

There is no general consensus among laparoscopic surgeons, if, and at what level would haptic feedback improve the quality of procedures. According to many surgeons, having visual feedback alone provides adequate information about the tissue palpation force for safe and reliable operation, however, the lack of haptic feedback is often considered as a major limitation in robot-assisted MIS procedures [56]. Clearly, an experienced surgeon finds the lack of haptic feedback less disturbing than a novice. However, in haptic guidance, learning spatiotemporal trajectories, contrary motion compensation (Fulcrum-effect), and strategy planning, the presence of haptic feedback and/or surgical simulators can enhance force skill learning for trainees [57].

Providing a complex and reliable perception for the operators of haptic devices could not only enhance intra-operative performance, but it may also become an essential tool in surgical training and pre-operative planning. In recent years, the use of surgical software simulators has largely increased, offering different training scenarios, anatomical variations, and conditions in the operating environment [58,59]. Using haptic devices, a new dimension opened in performance evaluation during procedures. Moreover, due to the complex mechanical behavior of soft tissues, augmented simulations require reference data from real surgical scenarios and should be tested by human operators to validate the usability of the virtual models [60].

The problem of distinguishing between soft tissues by testing their mechanical properties is often referred to as the cognitive role of haptic devices in simulation environments [61]. Today's surgical simulators that are using haptic interfaces are both relying on simple mechanical models of soft tissues and complex, parameterized finite element models. However, for enhancing real-time operation and focusing on the most representative mechanical effects, simple models are preferred in order to keep the transparency of the operation at maximum. Besides high computational requirements, using bilateral haptic devices and accounting for tissue dynamics can also handle issues arising from communication latency [62]. Stability and accuracy deterioration caused by latency and other external disturbances, such as contacting hard tissues or elastic tool deformation, can also be addressed using realistic soft tissue models. Their integration into model-based force control algorithms largely increases the robustness and reliability of robot-assisted interventions [63]. The integration of soft tissue properties to robot-assisted and virtual reality-based MIS procedures is an actively researched topic within the field of surgical robotics. Methods for acquiring useful measurement data use a combined experimental procedure of measuring tissue relaxation force under step-like tissue compression and force measurement during constant compression rate indentation input. Samur et al. proposed a method for tissue parameter estimation using a custom indenter during laparoscopic surgery by means of inverse finite element solution to estimate optimum values of nonlinear hyperelastic and elastic properties [64]. Beccani et al. developed a tool for intra-operative wireless tissue palpation, using a cylindrical palpation

probe and estimating local volumetric stiffness values, assuming linear elastic behavior of the tissue [65].

A deformable model based on nonlinear elasticity and the finite element method for haptic surgical simulators was proposed in [66], validated on real-time simulations of laparoscopic surgical gestures on virtual liver models. Trejos et al. suggested an augmented hybrid impedance control scheme to perform force control, providing model-based control background for a tactile sensing instrument in intra-operative tissue palpation [67]. Endoscopically guided, minimally invasive cannulation tasks were investigated by Wagner et al. to test the hypothesis that force feedback can improve surgical performance, finding that applied forces by surgeons can be decreased for those with adequate training background [68]. In [51], Tholey et al. developed an automated laparoscopic grasper with force feedback capability in order to aid the surgeons in differentiating tissue stiffness through the PHANToM (Sensable Technologies, Woburn, MA) haptic device. Participants were asked to differentiate between tissues, having provided visual and/or haptic feedback to complete the task.

Alternative approaches are also popular in general force feedback for laparoscopic training and procedures. Horeman et al. developed a training system that provided visual haptic feedback of the interaction forces during a procedure [69]. They found that providing haptic feedback through visual representation considerably improved the quality of the solved tasks. A detailed feasibility study of lung tumor detection using kinesthetic feedback was published by McCreery et al., creating an *ex vivo* experimental environment, modeling various tissue stiffness values, injecting agar into healthy tissues, and substituting haptic feedback with recorded force data [70].

10.5 SOFT TISSUE MODELS

A detailed investigation about the most widely used tool-tissue interaction models was published by Famaey and Sloten, sorting the soft tissue models into three distinguished categories:

- *Continuum mechanics-based* tissue models, utilizing concepts of finite element analysis (FEA) and continuum-mechanics approaches
- *Heuristic* models, which represent a combination of linear and/or nonlinear spring and damping elements
- *Hybrid* models, usually representing the combination of FEA/continuum mechanics-based and heuristic approaches [71]

It is a common view that continuum mechanics-based tissue models allow one to provide a realistic behavior description function during the tissue manipulation, although the vast computational requirements, the high complexity of the geometry, and the highly generic approach limit their usability in real-time surgical applications and simulation environments. On the other hand, heuristic models, which are also

often mentioned as rheological models or mass–spring–damper models, are proven to be useful in modeling basic surgical manipulation tasks, including indentation and tissue grabbing [72]. In many cases, mass–spring–damper models also provide an analytical solution to the problems, allowing a more straightforward mathematical description of the tool–tissue interaction phenomenon [3]. There is extensive literature about the description of soft tissue behavior both in fixed compression rate indentation [6] and tissue relaxation phases [73], providing raw measurement data on the force response. The use of heuristic models for soft tissue representation was deeply discussed by Yamamoto, listing and assessing numerous basic models during point-to-point palpation for hidden lump detection [7]. The mechanical properties of human adipose tissues were investigated by Alkhouli et al. using a viscoelastic linear soft tissue model, focusing on the stress relaxation phase of the indentation [74]. The nonlinear viscoelastic mass–spring–damper model created by Troyer et al. was also verified based on relaxation tests, bearing in mind that the model can be later integrated in FEA approaches in order to speed up the computational process [75].

In a wider perspective, the heuristic soft tissue models can be integrated into image-based surgical guidance systems, aiding accuracy and stability of the interventions [76], while applying them as visual cues, the performance of haptic feedback devices can also be improved significantly. A fine example of such virtual soft tissue models was presented by Li et al., introducing a pseudo-haptic feedback-based method for the investigation of embedded hard incisions in a silicone phantom tissue [77]. Another complex tissue model was proposed by Leong et al. [9], where a curve fitting method was proposed for the acquisition of the soft tissue mechanical parameters, based on measurement data from [78]. While the initial idea of Leong was feasible, the correct mathematical derivation of the results was missing. The corrected mathematical description, improved measurement data, and detailed model verification was presented by Takács et al., concluding that the proposed nonlinear Wiechert heuristic model can effectively model the soft tissue behavior and quantitatively represent its mechanical properties during basic surgical manipulation tasks [55]. A comprehensive overview of the structure and usability of heuristic tissue models was presented by Wang and Hirai [79]. They investigated the force response of different commercially available clay samples and Japanese sweets materials.

Soft tissue manipulation requires sophisticated techniques and precise surgical tools, particularly during tissue indentation, cutting, or suturing. There is a need for accurate soft tissue models, as the best performance of surgical robotic applications can only be achieved by utilizing control methods taking the tissue mechanical behavior and properties into account [16]. Furthermore, in terms of stability and transparent teleoperation, the accurate modeling of tool-tissue interaction is essential for utilizing reliable model-based control methods. The most important aspects of these model-based approaches becomes imminent in the case of force control. The reaction force during a given manipulation can be estimated, and the control signal, which directly sets the input force or the tool trajectory, can be calculated. The control signal is then transferred to the robotic arm holding or manipulating the soft tissue, increasing the efficiency, stability, and accuracy of the intervention.

10.6 METHODS FOR MODELING SOFT TISSUES

10.6.1 Mass–Spring–Damper Models

Let us consider the tool–tissue interaction model proposed by Leong et al. in [9]. As shown in Figure 10.2, mass–spring–damper models are uniformly distributed under the soft tissue surface. When the tissue surface is deformed, the total force response is calculated by adding up the force response values of each individual element, which are all infinitely small and are connected to the surface of the deformed tissue. The model assumes that the displacement of each point on the tissue surface is known at any time and the deformation is always happening in the axis of the mechanical element.

The heuristic soft tissue modeling approach is one of the simplest ways to model the behavior of soft tissues. The complex biological structure of these tissues induces unique and diverse mechanical properties for these materials, including high levels of inhomogeneity, viscoelasticity, and anisotropy, which cannot be overlooked and drastically simplified when designing robot control applications. These restrictions are usually not applied for everyday industrial and service robotics applications for material handling and machining.

The concept of this modeling approach is very simple: linear and/or nonlinear damper and spring elements are assembled together in a mixed parallel and serial connection. The assembled network of mechanical elements is typically used for describing the soft tissue behavior during uniaxial deformation, while projecting force values representing the reaction force response of the tissue. Nevertheless, the model can be extended for measurement of rheological and viscoelastic properties of multiaxial elongation as well [80].

Efficient application of this approach requires the knowledge of the $u(t)$ deformation input of each of the end points of the network of the combined mechanical elements. With this information in hand, the force response can be given by a closed-form mathematical function, called the force response function. The reaction force depends on the basic mechanical properties of the element.

- Linear spring elements represent a force response f_s, which is calculated from the specific spring stiffness coefficient k and the deformation magnitude in the spring axial direction:

$$f_s = k(x_1 - x_2). \tag{10.1}$$

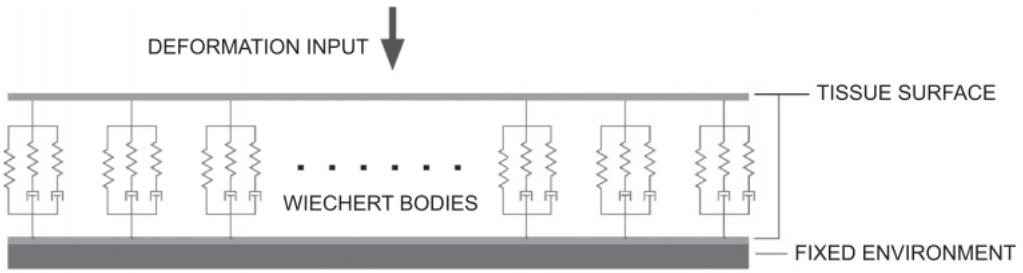

FIGURE 10.2 The proposed linear tool-tissue interaction model, where the Wiechert bodies are distributed along the tissue surface.

- Linear damper elements represent a force response f_d, which is calculated from the damping coefficient b and the relative deformation rate of the end points in the axial direction:

$$f_d = b(\dot{x}_1 - \dot{x}_2). \tag{10.2}$$

where x_1 and x_2 represent the end coordinates of the spring and damper elements, $\dot{x}_1$ and $\dot{x}_2$ are the deformation rates in the axial direction.

The literature of mass–spring–damper models lists three basic combinations of these elements in common application, referred to as the basic models of viscoelasticity. These are the Kelvin–Voigt, the Maxwell, and the Kelvin models, as shown in Figure 10.3 [72]. In this section, only the behavior of linear models is discussed, but the general description applies to the nonlinear models as well.

In analytical mechanics, the Kelvin–Voigt model is the most commonly used mass–spring–damper model, as it is capable of representing reversible deformation and stress relaxation simultaneously. The behavior of the system can be described using an ordinary differential equation and an analytical solution to the force response function can be given by solving this equation. The easy interpretation and simplicity of this approach makes it very popular in many fields of mechanical engineering. A strong limitation of the model arises from its difficulty of handling step-like deformations, as the reaction force on the damper element would be infinitely large in the case of a sudden deformation variation. As the Kelvin–Voigt model consists of the parallel connection of a spring and a damper element, the representation of the response function for the reaction force in the time domain can be written as:

$$f_{KV}(t) = b\dot{u}(t) + ku(t), \tag{10.3}$$

where $u(t)$ is the deformation function. The reaction force response function in the Laplace domain is:

$$F_{KV}(s) = (bs + k)U(s). \tag{10.4}$$

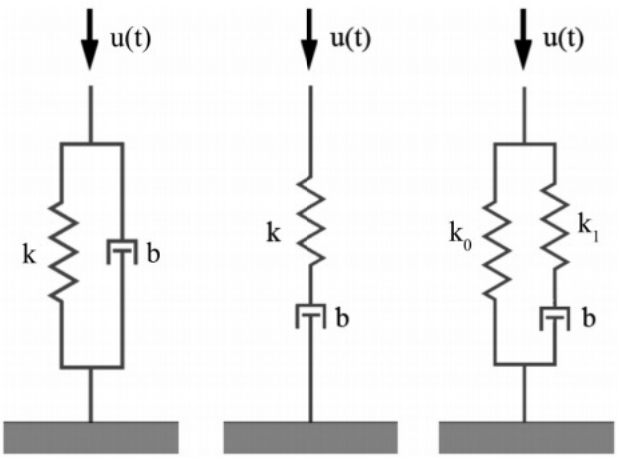

FIGURE 10.3 The most widely used viscoelastic models in soft tissue modeling: Kelvin–Voigt model (left), Maxwell model (center), and the Kelvin model (right).

In viscoelasticity, *creep* is a phenomenon that describes permanent deformation due to the applied mechanical stress, which can be straightforwardly modeled by the Maxwell model. In this approach, a spring and a damper element are connected in a serial way, representing creep and stress relaxation in the material. In practical applications, the use of this model is limited by the fact that the force response value converges to 0, when a constant deformation input is applied due to the serial connection of the damper element. The model is not capable of modeling residual stress and the deformation function of the model cannot be directly expressed as a function of the acting forces. This is due to the unknown position of the virtual mass point connecting the two elements, which can only be estimated but not directly measured. As time domain representation of this model generally does not exist, a Laplace domain description is given below:

$$F_M(s) = \frac{kbs}{bs+k} U(s). \tag{10.5}$$

The simplest possible solution to model residual stress, reversible deformation, and stress relaxation is provided by the Kelvin model, also often referred to as the Standard Linear Solid (SLS) viscoelastic model. The Kelvin model is constructed by the parallel connection of a single spring element and a Maxwell model. A popular time-domain representation is usually given in a closed-form formula:

$$f_K(t) + \frac{b}{k_1}\dot{f}_K(t) = k_0\left(u(t) + \frac{b}{k_0}\left(1 + \frac{k_0}{k_1}\dot{u}(t)\right)\right), \tag{10.6}$$

while in the Laplace domain, the transfer function of this model is given by:

$$F_K(s) = \frac{b(k_0+k_1)s + k_0k_1}{bs+k_1} U(s). \tag{10.7}$$

In modern medical technologies, the high diversity of the soft tissues and their complex behavior during manipulation tasks yielded to the need for more sophisticated viscoelastic models, relying on the modularity of the heuristic soft tissue modeling approach. Ultimately, new combinations of linear or nonlinear spring and damper elements would allow one to increase the performance of surgical robotics applications by better understanding the tissue behavior. Two of these more complex yet commonly used combinations are shown in Figure 10.4. If a Maxwell and a Kelvin model are connected serially, the so-called Maxwell–Kelvin model can be created, consisting of a total of five mechanical elements. The elastic behavior and relaxation properties can be more accurately modeled using this model, refining tissue parameters based on the experimental data using curve fitting. There exists a Laplace domain representation for this approach:

$$F_{MK}(s) = \frac{A_{2_{MK}}s^2 + A_{1_{MK}}s}{B_{2_{MK}}s^2 + B_{1_{MK}}s + B_{0_{MK}}} U(s), \tag{10.8}$$

where $A_{2_{MK}}$, $A_{1_{MK}}$, $B_{2_{MK}}$, $B_{1_{MK}}$, $B_{0_{MK}}$ are linear functions of the mechanical parameters k_0, k_1, k_2, b_1, and b_2.

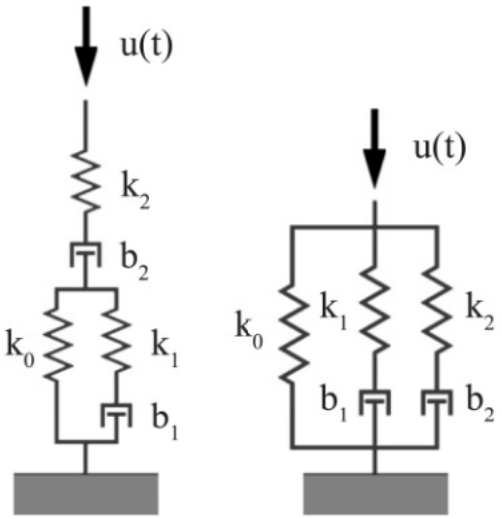

FIGURE 10.4 Advanced combinations of heuristic viscoelastic models in soft tissue modeling: the Maxwell–Kelvin model (left) and the Wiechert model (right).

More complex mass–spring–damper models do not necessary give better accuracy and performance in tissue behavior modeling. The Maxwell–Kelvin model, for example, will still have the limitation of the reaction force converging to 0, similar to the previously discussed Maxwell model. Alternatively, a Kelvin model and several Maxwell models can be connected in a parallel way in order to form a generalized Maxwell model, or, if there is only one Maxwell body connected to the system, the Wiechert model. It was shown in [9] and [55] that this assembly provides a smooth and accurate way for fine-tuning mechanical parameters for specific tissues during simple surgical manipulations.

A comparison of the Wiechert and Kelvin models was provided by Wang et al. [81], concluding that there is a significant advantage of using the Wiechert model in modeling spleen and liver organ force response estimation. A methodology for parameter estimation for the Wiechert model was also presented by Machiraju et al. [82], carrying out the investigation of tissue behavior during the stress relaxation phase. In the Laplace domain, the transfer function of the Wiechert model is as follows:

$$F_W(s) = \frac{A_{2_W} s^2 + A_{1_W} s + A_{2_W}}{B_{2_W} s^2 + B_{1_W} s + B_{0_W}} U(s) = W_W(s) U(s), \tag{10.9}$$

where

$$A_{2_W} = b_1 b_2 (k_0 + k_1 + k_2),$$

$$A_{1_W} = (b_1 k_2 (k_0 + k_1) + b_2 k_1 (k_0 + k_2),$$

$$A_{0_W} = k_0 k_1 k_2 b_2,$$

$$B_{2_W} = b_1 b_2,$$

$$B_{1_W} = b_1 k_2 + b_2 k_1,$$

$$B_{0_W} = k_1 k_2.$$

10.6.2 Data Collection Methods

The structured collection of experimental data was motivated by the lack of general, publicly available force measurement data from tissue palpation. A frequent approach for this type of data collection aims for the palpation or indentation of *ex-vivo* tissue samples with known compression speed, creating a set of tissue deformation–reaction force characteristics. The goal of these measurements is to provide a reference data for curve fitting, where its deviation in the force response of the simulated tissue behavior is minimized for the optimal set of tissue parameters of the investigated model. With these considerations in hand, the following methodology for tissue characterization using the Wiechert model was carefully planned in order to provide sufficient data for model verification. According to the tool-tissue interaction model, infinitely small Wiechert bodies are distributed under the deformed tissue surface as shown in Figure 10.2. The model parameters are obtained by applying a uniform deformation input on the surface. During the initial experiment, six pieces of cubic-shaped fresh beef liver samples were investigated, with edge lengths of 20 ± 2 mm. The dimensions of each of the specimens were measured before and after the indentation tests. The specimens were compressed at three fixed compression rates: a slow rate of 20 mm/min, a medium rate of 100 mm/min, and a near-step input at 750 mm/min, the latter being the maximum deformation rate provided by the physical system. The indentation tests were carried out at the Austrian Center for Medical Innovation and Technology (ACMIT, Wiener Neustadt), on a Thümler GmbH TH 2730 tensile testing machine connected to an Intel Core i5-4570 CPU with 4 GB RAM, using ZPM 251 (v4.5) software. The force response data was collected with an ATI Industrial Automation Nano 17 titanium six-axis Force/Torque transducer, using the 9105-IFPS-1 DAQ Interface and the power supply at 62.5 Hz sampling time. An Intel Core i7-2700 CPU with 8 GB RAM hardware and the ATICombinedDAQFT .NET software interface was used for data visualization and storage. In the case of each specimen (marked by letters A–F), at first, the low and medium speed indentation tests were carried out, reaching 4 mm of indentation depth. The deformation input function was also recorded for validation purposes.

The uniform surface deformation was achieved by using a custom designed 3D-printed indenter head mounted on the force sensor. The starting position of the indenter was 1 mm above the surface of the specimen. During the evaluation of the measurement data, only 3.6 mm of indentation depth was investigated. This way, any nonlinearity in the ramp-input function during the compression could be filtered out. For the constant compression rate indentation test, force data was recorded during the head movement and each of the specimens was subjected to compression 12 times. The reaction force response curves did not have any systematic deviation from the first test on the same specimen. This strengthens the assumption that no substantial tissue damage was caused during the measurements that could have a depriving effect on the final results. The near-step input deformation was applied several times on each of the specimens. Evaluating the measurement data, it was found that the force response magnitude in the relaxation phase (60 seconds) decreased significantly during the second and third experiments on the same tissue, most likely from the severe damage to the internal tissue structure. Based on this observation, only the very

first set of measured data points was used for the parameter estimation in the relaxation phase for each specimen. The image of the experimental setup is shown in Figure 10.5.

10.6.3 Indentations Tests

In the first phase, the force response data from the relaxation tests was evaluated. This way, an initial estimation can be given on the individual mechanical parameters of the linear Wiechert model. For the simplification of the calculations, the indentation speed of 750 mm/min was approximated with a step-input function. The analytical expression for the force response function can be easily obtained by taking the inverse Laplace transform of Eq. (10.9). In the Laplace domain, the output function is calculated by taking the product of the transfer function $W_W(s)$ and the Laplace transform of the step-input function:

$$f_{W_r}(t) = L^{-1}\left\{W_W(s)\frac{x_d}{s}\right\} = x_d\left(k_0 + k_1\left(1 - e^{-\frac{k_1}{b_1}t}\right) + k_2\left(1 - e^{-\frac{k_2}{b_2}t}\right)\right), \tag{10.10}$$

where $f_{W_r}(t)$ is the reaction force in the relaxation phase and $x_d = 4$ mm is the compression depth at the maximum deformation. For all six specimens, the relaxation data is displayed in Figure 10.6. The average response curves are also shown in Figure 10.6 for better visualization, which were obtained by taking the average values of the response data for each of the specimens, weighted with respect to the tissue surface size, and normalized to 20×20 mm. An unexpected break can be observed in the curves for tissue samples, which is supposedly due to the effect of the deceleration of the indenter reaching the target indentation depth. For simplification reasons, this break is not taken into account during the curve fitting phase, as it does not affect the force response results significantly. The most relevant sections of the response curves are the initial relaxation slopes (force relaxation)

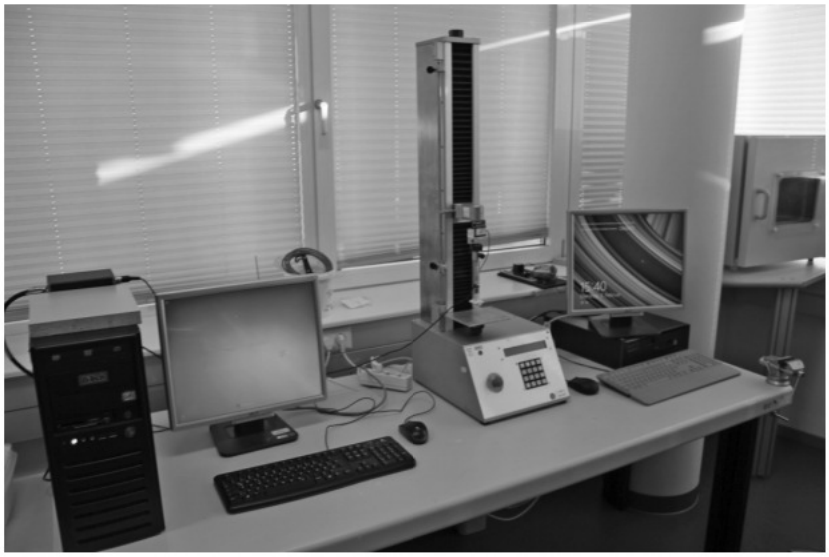

FIGURE 10.5 Experimental setup for beef liver indentation tests at the Austrian Center for Medical Innovation and Technology (ACMIT).

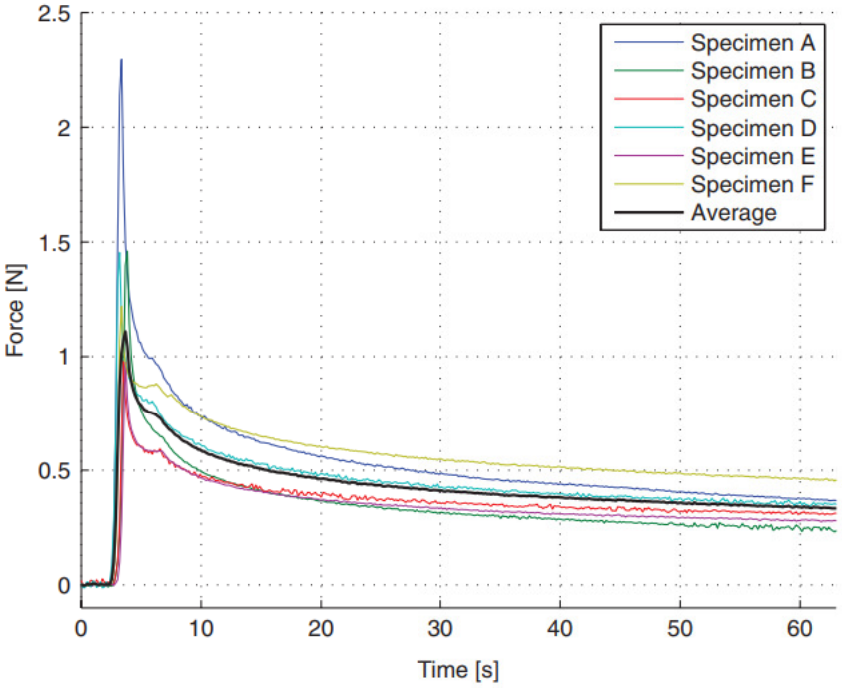

FIGURE 10.6 Force response curves for step-input relaxation tests for eight identically cut liver pieces.

and the steady-state values (residual stress). As previously derived, a closed-form solution to the step-input can given and curve fitting on the original measurement can be applied. MATLAB® *cftool* toolbox was used for carrying out the curve fitting, while the parameters were independently obtained for each of the six specimens and were compensated by the tissue surface magnitude. Summarizing, the procedure resulted in six sets of parameters of stiffness and damping parameter values:

$$k_i^c = k_i \frac{A_0}{A}, i = 1,2,3 \tag{10.11}$$

$$b_j^c = b_j \frac{A_0}{A}, j = 1,2, \tag{10.12}$$

where A is the surface area of each specimen and $A_0 = 400$ mm^2 is the reference tissue surface value. The average parameter values are listed in Table 10.1 under the *linear* model type.

TABLE 10.1 Parameter Estimation Results from Force Relaxation and Constant Compression Rate Tests

Model Type	K_0 [N/m]	K_1 [N/m]	K_2 N/m]	b_1 [Ns/m]	b_2 [Ns/m]	k_0 [m^{-1}]	k_1 [m^{-1}]	k_2 [m^{-1}]	RMSE *Combined* [N]
Linear	4.86	57.81	53.32	9987	10464	–	–	–	0.1865
Nonlinear	2.03	0.438	0.102	5073	39.24	909.9	1522	81.18	0.0206

It was shown in [83] that the Wiechert model gives a reasonably good description of the soft tissue behavior in the relaxation phase. However, the verification of the model requires more indentation scenarios, which were based on two more sets of compression tests with constant compression rate. The average force response curves for each specimen for the case of 20 mm/min and 100 mm/min are displayed in Figures 10.7 and 10.8, respectively, along with the global weighted average response curve. Note that for better visualization, the curves are displayed in an *indentation depth–force* graph instead of the previously used *time–force* graph. The indentation depth was 4 mm. The figures only show the first 3.6 mm of deformation for previously discussed reasons. Utilizing the same method for obtaining the analytical force response as it was used in the step-input case, the following analytical expression was obtained for the force response:

$$f_{W_c}(t) = L^{-1}\left\{W_W(s)\frac{v}{s^2}\right\} = v\left(k_0 t + b_1\left(1 - e^{-\frac{k_1}{b_1}t}\right) + b_2\left(1 - e^{-\frac{k_2}{b_2}t}\right)\right), \tag{10.13}$$

where v denotes the compression rate (20 mm/min or 100 mm/min) and f_{W_c} stands for the force response magnitude. Theoretically, the substitution of the model parameters into Eq. (10.13) should give a good estimation on the measurement data for the force curves. It is important to note that the 750 mm/min indentation speed was approximated as a step-input, therefore, a minor compensation of the previously obtained mechanical parameters would still be needed. However, the constant compression rate indentation test results showed that the qualitative behavior of the analytical response curve largely differs from the measured response curve. Therefore, the validity of the linear Wiechert model in this

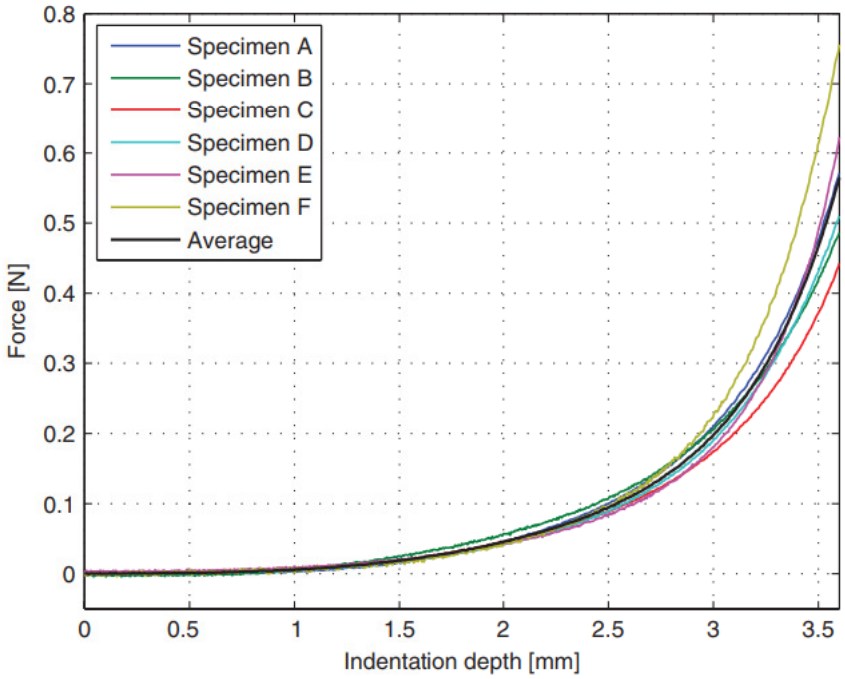

FIGURE 10.7 Force response curves for constant compression rate indentation tests at 20 mm/min.

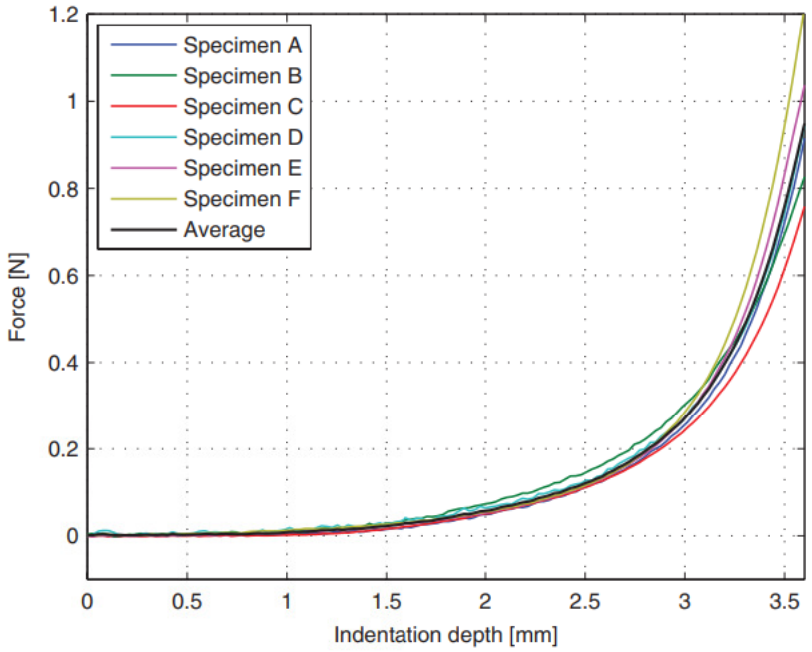

FIGURE 10.8 Force response curves for constant compression rate indentation tests at 100 mm/min.

indentation phase is limited, while from the haptics application point of view, it is more relevant to have a good soft tissue model during constant compression rate indentation. The estimated response curves and the average measurement data for the constant compression rate of 100 mm/min are shown in Figure 10.9. The best fitting curve derived by the MATLAB® *cftool* toolbox, assuming positive mechanical parameter values, is also displayed in Figure 10.9.

The measurement data and the considerable deviation from the estimated force response implies that the reaction force during constant compression rate indentation represents progressive stiffness characteristics, contrary to the previously assumed linear one. The phenomenon is a direct consequence of the complex biomechanical structure of the liver tissue, which cannot be observed during step-response relaxation tests. There is a need for the extension of the model, keeping it as simple as possible. A possible way for addressing progressing stiffness characteristics is to introduce nonlinearities through the spring elements. A model as such, with some basic restrictions is introduced, based on several practical considerations:

$$k_i(x) \geq 0, \tag{10.14}$$

$$\frac{dk_i(x)}{dx} \geq 0, \tag{10.15}$$

for all $x > 0$ and $i = 1,2,3$. This implies that both the stiffness values and their derivatives with respect to the indentation depth must be nonnegative. The proposed nonlinear stiffness function is the following:

$$k_j(x) = K_j e^{\kappa_j x} \tag{10.16}$$

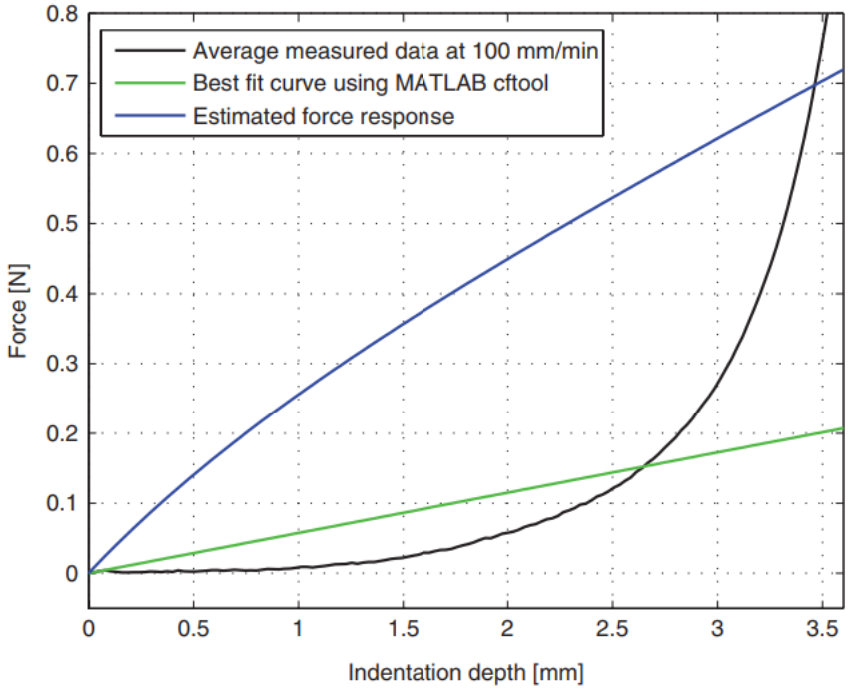

FIGURE 10.9 Verification results of the linear Wiechert model at the compression rate of 100 mm/min. The blue curve shows the predicted force response from the parameter data acquired from relaxation tests, while the measured force response is represented by the black curve. The green curve corresponds to the best fit using reasonable mechanical parameters, clearly indicating that the model is not capable of predicting the reaction force in the case of constant compression rates.

for $j = 1,2,3$, where K_j and k_j are nonnegative constants. In the proposed model, all of the three spring elements have the same exponential, nonlinear behavior. Damping elements remain linear. This representation introduces a total of eight mechanical parameters, creating an off-the-shelf model that could be used both in compression and relaxation phases.

Summarizing the findings, the experimental data indicates that the force response is a convex curve in the case of constant compression rate indentation. Figure 10.9 shows that because of the nature of Eq. (10.13), the linear Wiechert model would always estimate a concave force response curve. The proposed nonlinear Wiechert model addresses this issue by introducing progressive, exponential spring element stiffness, which, logically, would lead to a better fit with the experimental data.

10.6.4 The Proposed Nonlinear Mass–Spring–Damper Model

The nonlinear formulation of the proposed soft tissue model does not allow a closed-form analytical expression for the force response. Therefore, instead of applying the MATLAB® *cftool* toolbox, the *fminsearch* optimization function was used to find the optimal set of tissue parameters [84]. The parameter values and the combined root mean square error results for fitting the experimental data are shown in Table 10.1. The curve fitting procedure was carried out simultaneously on both datasets of 20 mm/min and 750 mm/min

responses, while the combined error values were calculated by summing up the individual root mean square error (RMSE) for each curve, defining the cost function for *fminsearch*. The estimated force responses, utilizing the parameters from Table 10.1, are shown in Figures 10.10 and 10.11.

Independent parameter verification was carried out by simulating the force response during the constant compression indentation rate of 100 mm/s. During the simulation, the following set of differential equations was solved:

$$\begin{aligned} \dot{x}_0 &= v(t), \\ \dot{x}_1 &= \frac{1}{b_1} K_1 (x_0 - x_1) e^{\kappa_1 (x_0 - x_1)}, \\ \dot{x}_2 &= \frac{1}{b_2} K_2 (x_0 - x_2) e^{\kappa_2 (x_0 - x_2)}, \end{aligned} \tag{10.17}$$

where $v(t)$ is the surface deformation rate, x_0 denotes the position of an arbitrary point at the surface, while x_1 and x_2 represent two virtual points, connecting k_1–b_1 and k_2–b_2 elements, respectively, as shown in Figure 10.12. The system output is the reaction force, $F(t)$, calculated by:

$$F(t) = K_0 x_0 e^{\kappa_0 x_0} + K_1 (x_0 - x_1) e^{\kappa_1 (x_0 - x_1)} + K_2 (x_0 - x_2) e^{\kappa_2 (x_0 - x_2)}. \tag{10.18}$$

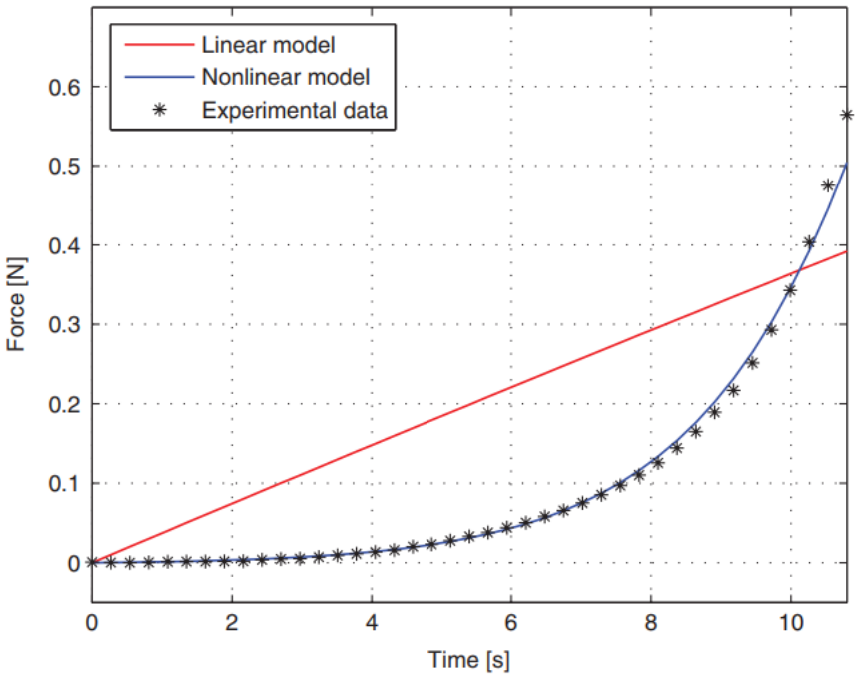

FIGURE 10.10 Force response estimation curves, utilizing the parameter sets from Table 10.1 at a constant compression rate of 20 mm/s.

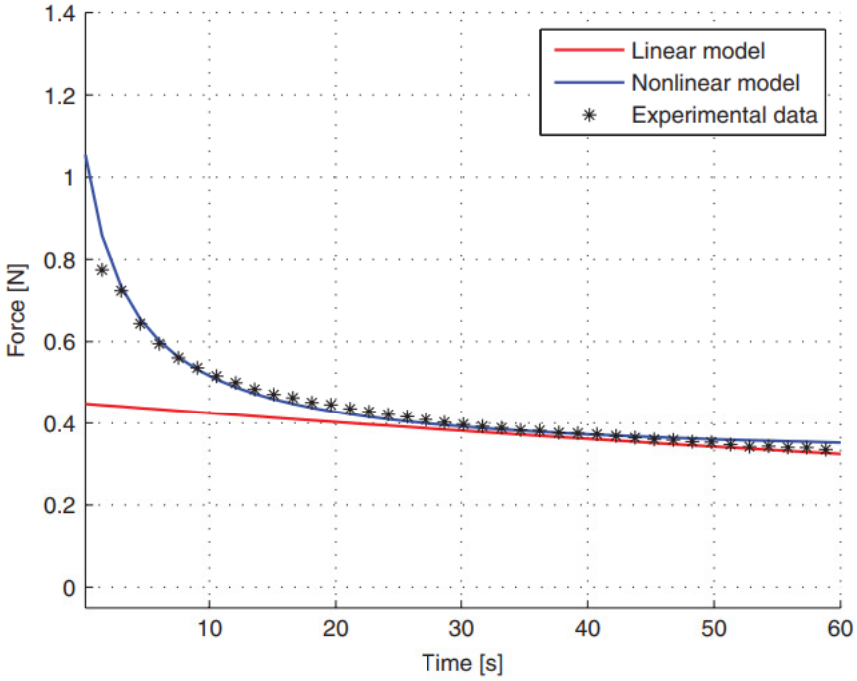

FIGURE 10.11 Force response estimation curves, utilizing the parameter sets from Table 10.1, in the case of a step-like input, focusing on stress relaxation data.

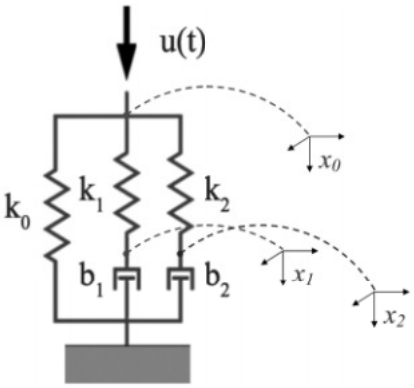

FIGURE 10.12 The proposed nonlinear soft tissue model, with the indication of the virtual mass points.

10.7 RESULTS

Figure 10.13 shows how the simulation results are mapped on the measurement data. The average RMSE was calculated separately with respect to each of the specimens, resulting with $\varepsilon_{RMSE} = 0.1748$ [N]. This proves that the model represents the tissue behavior under the given manipulation tasks very well. The simulated curve yielded a somewhat lower reaction force value than those of the experimentally obtained, which is an expected behavior. During the parameter estimation, an ideal step-response curve was used as an input function in the simulation, while, during the indentation tests, the maximum indentation speed was 750 mm/min. As a consequence, the lower-than-desired indentation speed resulted in lower stiffness values for the spring elements, partly due to the rapid relaxation during the

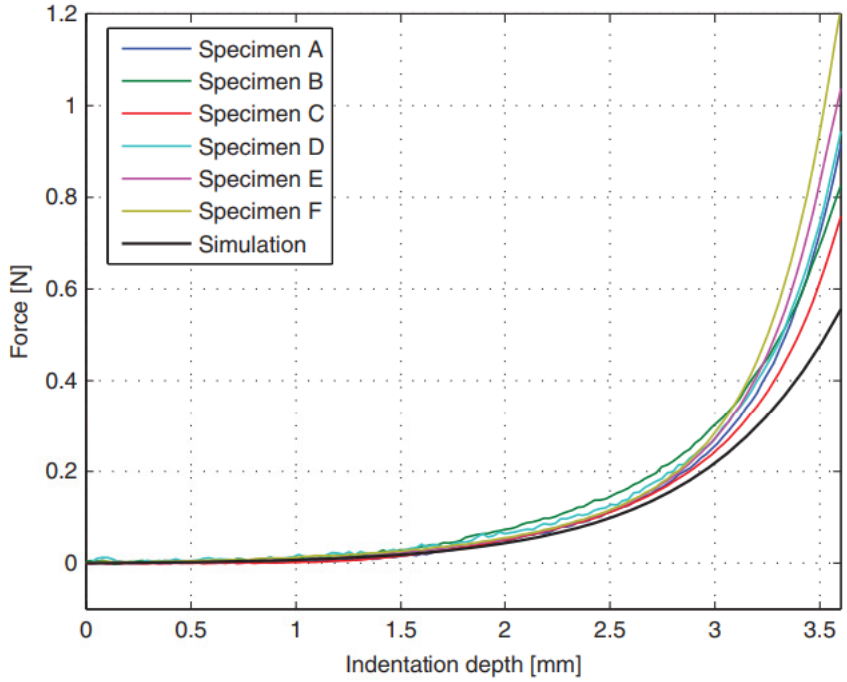

FIGURE 10.13 Force response curves for constant compression rate indentation tests at 100 mm/min, showing the simulated response of the nonlinear model using the parameters listed in Table 10.1.

compression phase. The effect can be observed in both Figure 10.10 and Figure 10.13. This does not affect the validity of the model significantly, as the qualitative behavior is still satisfying in all the simulated cases.

10.7.1 Model Verification Methods

The verification of the approach was extended to the scenario of nonuniform surface deformation, utilizing the basic concept shown in Figure 10.2. Additional experimental data was collected from indentation tests, where 3 specimens with the dimensions of $25 \times 25 \times 200$ mm from the same beef liver were palpated with a sharp instrument, taking special care not to physically damage the tissue surface. Constant rate indentations were carried out at four different indentation rates (5 mm/s, 10 mm/s, 20 mm/s, and 40 mm/s) at different points of the surface of each specimen, reaching 6 mm of indentation depth. The indenter used for the experiments was a 3D-printed piece that was mounted on the flat instrument used in the experiments for the uniform deformation. At the tip, the indenter had a bevel angle of 30° and its length was 30 mm. It was assumed that the indenter created a line-like deformation input on the surface of the specimens, perpendicular to their longest dimensions. The schematic figure of the nonuniform indentation is shown in Figure 10.14.

A few assumptions have been made prior to the verification of the estimation of the reaction force:

- the surface deformation shape is approximated as a quadratic function and is uniform along the width of the specimen

- it is assumed that the indentation only affects the liver structure in a certain ρ distance from the indentation point
- only uniaxial deformation is considered, therefore, all nonvertical forces are neglected in the calculations

The reaction force was assumed to be the sum of the reaction of infinitely small elements over the tissue surface:

$$F(t) = \iint_{y,z} f(y,z,t)dydz, \tag{10.19}$$

where $f(y,z,t)$ is the force response of a single infinitely small element at the surface point (y,z) at a given time t. $f(y,z,t)$ can be calculated by solving Eq. (10.18) for each surface element using the unique deformation rate $v_{x,y}(t)$ of the element and utilizing *specific* stiffness and damping values shown in Table 10.2. These specific values were obtained by normalizing the appropriate parameters to the surface size of 1 m^2.

The surface of the tissue was discretized using square-shaped cells $A_i = A_{y_i,z_i}$ with the edge length of 0.1 mm. The deformation rate profiles for each element, $v_i(t)$, were obtained from visual recordings. The indentation tests were recorded by a conventional video camera, fixed along the z-axis. The dislocation of seven surface points was tracked by analyzing 12 video files frame-by-frame at time intervals of 1 s. The resolution of the picture was 1980 × 1980 pixels, the recordings were taken at 25 frames per second. An average deformation profile was calculated by processing the data manually. It was found that a quadratic function was a good approximation for the final deformation surface (after reaching the $x_d = 6$ mm indentation depth), assuming that the deformation surface is symmetrical to the axis of indentation. Doming effects were neglected during the indentation, as these effects are more relevant at the regions far from the indentation point. Due to the progressive spring characteristics of the model, these regions contribute very little to the overall force

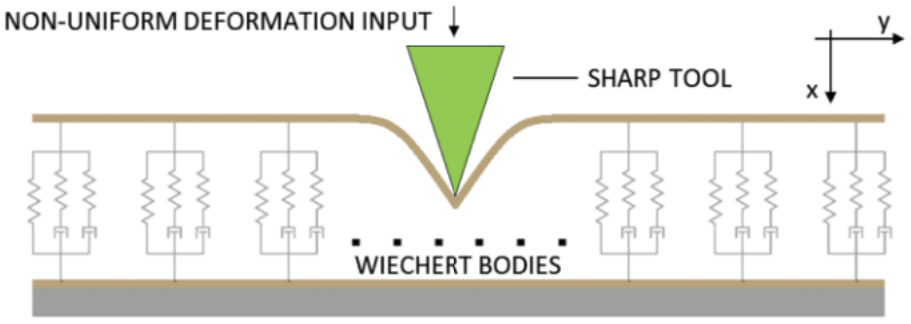

FIGURE 10.14 The schematic figure of the nonuniform indentation tests.

TABLE 10.2 Specific Parameter Values for the Use of Nonuniform Surface Deformation Model Verification

K_0^s [N/m³]	K_1^s [N/m³]	K_2^s [N/m³]	b_1^s [Ns/m³]	b_2^s [Ns/m³]	κ_0 [m^{-1}]	κ_1 [m^{-1}]	κ_2 [m^{-1}]
5075	1095	255	$127 \cdot 10^6$	$1.1 \cdot 10^6$	909.9	1522	81.189

response. With the assumptions above, the deformation rate profile $v_i(t)$ can be obtained at each surface point A_i, provided by the following equation:

$$v(y,t) = \frac{v_{in}}{\rho^2}(|y| - \rho)^2, \tag{10.20}$$

indicating that in the case of constant indentation rate, each surface point is moving at a constant speed. Eq. (10.18) was solved for each element and the force response was obtained and summed using the velocity profiles according to Eq. (10.20).

10.7.2 Model Verification Results

The estimated force response and the results of the simulation for the third specimen at 10 mm/min indentation speed are shown in Figure 10.15. Calculations were carried out on an Intel Core i5-3337U CPU with 8 GB RAM, the simulation time varied between 0.5 and 1.5 s, depending on the indentation speed, and thus, the length of the experiment. Based on the results and the low RMSE values, it can be concluded that the method can be used in applications for real-time force estimation. As shown in Figure 10.15, the experimentally obtained force response curves initially follow the simulated curve reasonably well, both qualitatively and quantitatively (region A). At the indentation depth of 4 mm, the slope of the experimental curves increases rapidly, which is assumed to be due to the tension forces arising in the normal direction with respect to the indentation axis (region B). This is an expected behavior, indicating that at higher deformation levels, the 1 DoF approach of the problem should be handled with caution. The RMSE values for each verification case were computed, with the results varying between $\varepsilon_{\text{RMSE,min}} = 1.384$ N and $\varepsilon_{\text{RMSE,max}} = 2.821$ N. The proposed soft tissue model can also be extended to more complex

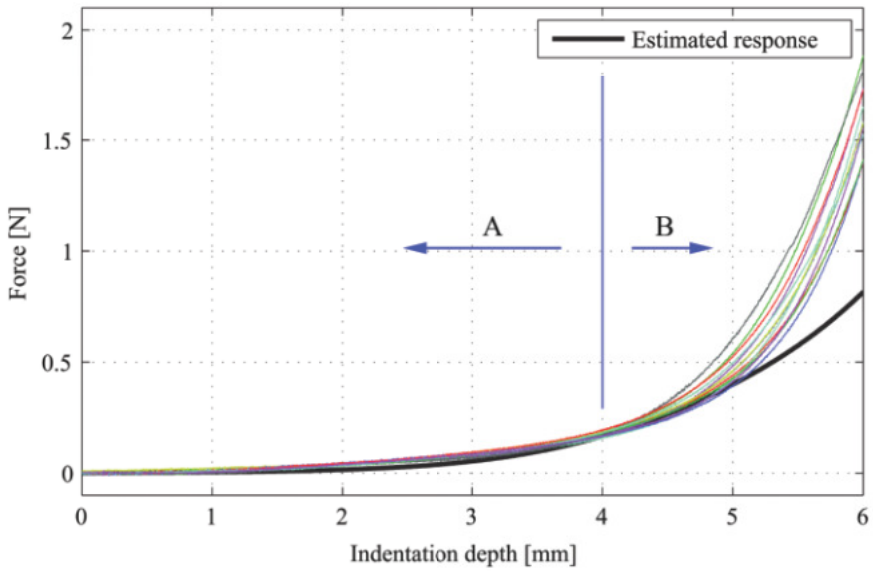

FIGURE 10.15 Measurement results and estimated force response for the case of 10 mm/min indentation for nonuniform surface deformation. The model fits the experimental data very well in region A, while in region B, this approach should be used with care.

surface deformation functions. Given that the boundary conditions are well-defined, one would find finite element modeling methods a useful tool for determining the surface deformation shape function [12].

10.8 USABILITY OF THE PROPOSED MODEL

The model proposed in this chapter can be integrated in a control scheme and the corresponding control design methodology, presented by Takács et al. in [85], regulates interaction force during autonomous manipulation of soft biological tissues. This approach gives an extensive application example for utilizing recent results of polytopic model-based control through the framework of Tensor Product Model Transformation [86]. Control of the reaction force during robotic interaction with soft tissues, for example, grasp–hold–release cycles, still remains an actively researched topic. Since biological tissues typically have highly nonlinear dynamic behavior (progressive stiffness characteristics, stress relaxation, etc.), time invariant linear controllers cannot provide ideal performance across the whole operation domain.

Based on the presented tissue model, parameter-dependent error dynamics can be utilized and system reformulation can be carried out in order to avoid the error rendered by the slow dynamics of one state variable [87]. Reformulating the system allows concentrating the 8-parameter dependency into a single parameter for a given application domain, constructing a feed forward term for the equilibrial input. The formulation opens up new possibilities in state feedback controller design, handling the unmodeled dynamics and further disturbances. Since the nonlinear model includes state variables that cannot be measured in the real process, the proposed tissue model can be also used as reference tissue model. This allows a linear matrix inequality (LMI)-based synthesis providing the variable gains as parameter dependent polytopic tensor product (TP) functions. The implementation of the proposed method into supervised telemanipulation/telesurgical equipment enhances the performance of these systems, allowing haptic sensing to the operator.

Along with force control, the problem of haptic feedback in telesurgical systems remains an open challenge in the related fields of research. Current surgical teleoperation systems lack any haptic feedback capabilities, limiting their usability in everyday practice. Furthermore, by allowing haptic feedback from manipulated real tissue, functionality can be extended to surgical simulation using virtual tissue models created by the proposed soft tissue modeling method.

Results of our usability study showed that the proposed nonlinear tissue model mimics the mechanical behavior of the *ex-vivo* tissue very well both from the qualitative and quantitative point of view. This allows the integration of the model into virtual tissue models used in surgical simulators—virtual environments providing physical interaction with the human operator through the haptic interface—where it is critical to have a realistic haptic sensation reflected to the human operator when manipulating the tissues. This way, the quality of HRI during surgical procedures can be improved, while accuracy, stability, and thus, safety, can be increased during procedures, as shown in other parallel studies as well [88]. The study also showed that using a haptic interface made it hard to distinguish

between artificial silicone tissues and real tissues during teleoperation, indicating that by creating a silicone sample according to the guidelines presented in this work, surgical training can be accelerated and enhanced by artificial tissue phantoms, yet providing realistic haptic sensation to the trainees, emphasizing the importance of introducing the concept of HRI in early medical and surgical education.

10.9 DISCUSSION

The importance of HRI in modern surgical systems is growing. In order to achieve a stable and reliable teleoperation in today's intervention systems, it is crucial to understand the mechanical behavior of manipulated tissues. Creating models for tool-tissue interaction and soft tissues can also aid model-based control methods. There is an extensive literature on various soft tissue models, however, the verification of heuristic models is mostly limited to stress relaxation tests. While the linear forms of these models are very popular in tissue behavior investigation, their practical usability is limited in general manipulation scenarios. The proposed model addressed this issue by accounting for the progressive stiffness characteristics of soft tissues, while a verification methodology was proposed using uniaxial compression tests, allowing its integration into robot-assisted surgical systems. It is important to note that lateral tension forces and their effect are not modeled in this approach, however, a quantitative representation of tissue behavior is still possible in cases of relatively small deformations. A reliable estimation of the reaction forces during telesurgical manipulation and the possibility of haptic feedback based on this model can increase the performance, accuracy, and safety of these procedures, therefore, current results open up new possibilities to a generic, uniform representation of soft tissues and artificial tissue samples, leading to more sophisticated tool–tissue interaction models representing a fine example of HRI in the medical field.

ACKNOWLEDGMENT

Authors acknowledge the financial support of this work by the Hungarian State and the European Union under the EFOP-3.6.1-16-2016-00010 project. T. Haidegger is supported through the New National Excellence Program of the Ministry of Human Capacities. T. Haidegger is a Bolyai Fellow of the Hungarian Academy of Sciences.

REFERENCES

1. Mathias Hoeckelman, Imre Rudas, Paolo Fiorini, Frank Kirchner, and Tamas Haidegger. Current capabilities and development potential in surgical robotics. *International Journal of Advanced Robotic Systems*, 12(61):1–39, 2015.
2. Nele Famaey and Jos Vander Sloten. Soft tissue modelling for applications in virtual surgery and surgical robotics. *Computer Methods in Biomechanics and Biomedical Engineering*, 11(4):351–366, 2008.
3. Árpád Takács, Sandor Jordan, Radu-Emil Precup, Levente Kovács, József Tar, Imre Rudas, and Tamás Haidegger. Review of tool-tissue interaction models for robotic surgery applications. In *Applied Machine Intelligence and Informatics (SAMI), 2014 IEEE 12th International Symposium on*, pp. 339–344, IEEE, Herl'any, Slovakia,January 2014.
4. Mahdi Tavakoli and Robert D Howe. Haptic effects of surgical teleoperator flexibility. *The International Journal of Robotics Research*, 28(10):1289–1302, 2009.

5. Cagatay Basdogan, Suvranu De, Jung Kim, Manivannan Muniyandi, Hyun Kim, and Mandayam A Srinivasan. Haptics in minimally invasive surgical simulation and training. *IEEE Computer Graphics and Applications*, 24(2):56–64, 2004.
6. Yidong Bao, Dongmei Wu, Zhiyuan Yan, and Zhijiang Du. A new hybrid viscoelastic soft tissue model based on meshless method for haptic surgical simulation. *The Open Biomedical Engineering Journal*, 7:116, 2013.
7. Tomonori Yamamoto. *Applying Tissue Models in Teleoperated Robot-Assisted Surgery*. PhD Dissertation, Johns Hopkins University, Baltimore, 2011.
8. Tomonori Yamamoto, Niki Abolhassani, Sung Jung, Allison M Okamura, and Timothy N Judkins. Augmented reality and haptic interfaces for robot-assisted surgery. *The International Journal of Medical Robotics and Computer Assisted Surgery*, 8(1):45–56, 2012.
9. Florence Leong, Wei-Hsuan Huang, and Chee-Kong Chui. Modeling and analysis of coagulated liver tissue and its interaction with a scalpel blade. *Medical & Biological Engineering & Computing*, 51(6):687–695, 2013.
10. Chao Liu, Pedro Moreira, Nabil Zemiti, and Philippe Poignet. 3D force control for robotic-assisted beating heart surgery based on viscoelastic tissue model. In *Engineering in Medicine and Biology Society, EMBC, 2011 Annual International Conference of the IEEE*, pp. 7054–7058, IEEE, Boston, MA, USA September 2011.
11. Orcun Goksel, Septimiu E Salcudean, and Simon P Dimaio. 3D simulation of needle-tissue interaction with application to prostate brachytherapy. *Computer Aided Surgery*, 11(6): 279–288, 2006.
12. Sarthak Misra, Kyle B Reed, Benjamin W Schafer, KT Ramesh, and Allison M Okamura. Mechanics of flexible needles robotically steered through soft tissue. *The International Journal of Robotics Research*, 29(13): 1640–1660. 2010.
13. Mohsen Mahvash and Pierre E Dupont. Mechanics of dynamic needle insertion into a biological material. *IEEE Transactions on Biomedical Engineering*, 57(4):934–943, 2010.
14. Sina Nia Kosari, Srikrishnan Ramadurai, Howard Jay Chizeck, and Blake Hannaford. Robotic compression of soft tissue. In *Robotics and Automation (ICRA), 2012 IEEE International Conference on*, pp. 4654–4659, Saint Paul, MN, USA, IEEE, May 2012.
15. ISO ISO. 10218-2: 2011: Robots and robotic devices—safety requirements for industrial robots—part 2: Robot systems and integration. Geneva, Switzerland: International Organization for Standardization, 2011.
16. Tamás Haidegger, Levente Kovács, Radu-Emil Precup, Balázs Benyó, Zoltán Benyó, and Stefan Preitl. Simulation and control for telerobots in space medicine. *Acta Astronautica*, 81(1):390–402, 2012.
17. Alex Ellery. Survey of past rover missions. In *Planetary Rovers*, pp. 59–69. Springer, Berlin2016.
18. Seunghwan Park, Yu-Cheol Lee, and Gon-Woo Kim. Implementation of spatial visualization for a tele-operated robot in a complex and hazardous environment. In *2014 IEEE International Conference on Automation Science and Engineering (CASE)*, pp. 285–289, Taipei, Taiwan August 2014.
19. John K Chapin, Karen A Moxon, Ronald S Markowitz, and Miguel AL Nicolelis. Real-time control of a robot arm using simultaneously recorded neurons in the motor cortex. *Nature Neuroscience*, 2(7):664–670, 1999.
20. Ren C Luo and Tse Min Chen. Development of a multi-behavior based mobile robot for remote supervisory control through the internet. *IEEE/ASME Transactions on Mechatronics*, 5(4):376–385, 2000.
21. Jaeheung Park and Oussama Khatib. A haptic teleoperation approach based on contact force control. *The International Journal of Robotics Research*, 25(5–6):575–591, 2006.
22. Shahin Sirouspour and Ali Shahdi. Model predictive control for transparent teleoperation under communication time delay. *IEEE Transactions on Robotics*, 22(6):1131–1145, 2006.

23. Ian Lenz, Ross Knepper, and Ashutosh Saxena. Deepmpc: Learning deep latent features for model predictive control. In *Robotics Science and Systems (RSS)*, pp. 1–9, 2015.
24. Dale A Lawrence. Stability and transparency in bilateral teleoperation. *IEEE Transactions on Robotics and Automation*, 9(5):624–637, 1993.
25. Ilia G Polushin, Peter X Liu, and Chung-Horng Lung. A force-reflection algorithm for improved transparency in bilateral teleoperation with communication delay. *IEEE/ASME Transactions on Mechatronics*, 12(3):361–374, 2007.
26. Peter F Hokayem and Mark W Spong. Bilateral teleoperation: An historical survey. *Automatica*, 42(12):2035–2057, 2006.
27. G Jagannath Raju, George C Verghese, and Thomas B Sheridan. Design issues in 2-port network models of bilateral remote manipulation. In *1989 IEEE International Conference on Robotics and Automation*, pp. 1316–1321, IEEE, Scottsdale, AZ, USA, May 1989.
28. Gary MH Leung, Bruce A Francis, and Jacob Apkarian. Bilateral controller for teleoperators with time delay via μ-synthesis. *IEEE Transactions on Robotics and Automation*, 11(1):105–116, 1995.
29. Homayoon Kazerooni, T-I Tsay, and Karin Hollerbach. A controller design framework for telerobotic systems. *IEEE Transactions on Control Systems Technology*, 1(1):50–62, 1993.
30. Shahin Sirouspour. Modeling and control of cooperative teleoperation systems. *IEEE Transactions on Robotics*, 21(6):1220–1225, 2005.
31. Wen-Hong Zhu and Septimiu E Salcudean. Stability guaranteed teleoperation: An adaptive motion/force control approach. *IEEE Transactions on Automatic Control*, 45(11):1951–1969, 2000.
32. József K Tar, János F Bitó, Imre J Rudas, Kristóf Eredics, and José A Tenreiro Machado. Comparative analysis of a traditional and a novel approach to model reference adaptive control. In *International Symposium on Computational Intelligence and Informatics (CINTI)*, pp. 93–98, Budapest, Hungary IEEE, November 2010.
33. Dongjun Lee and Perry Y Li. Passive bilateral control and tool dynamics rendering for nonlinear mechanical teleoperators. *IEEE Transactions on Robotics*, 21(5):936–951, 2005.
34. Jee-Hwan Ryu, Dong-Soo Kwon, and Blake Hannaford. Stable teleoperation with time-domain passivity control. *IEEE Transactions on Robotics and Automation*, 20(2):365–373, 2004.
35. Keyvan Hashtrudi-Zaad and Septimiu E Salcudean. Transparency in time-delayed systems and the effect of local force feedback for transparent teleoperation. *IEEE Transactions on Robotics and Automation*, 18(1):108–114, 2002.
36. Takashi Imaida, Yasuyoshi Yokokohji, Toshitsugu Doi, Mitsushige Oda, and Tsuneo Yoshikawa. Ground-space bilateral teleoperation of ets-vii robot arm by direct bilateral coupling under 7-s time delay condition. *IEEE Transactions on Robotics and Automation*, 20(3):499–511, 2004.
37. Hubert Baier and Günther Schmidt. Transparency and stability of bilateral kinesthetic teleoperation with time-delayed communication. *Journal of Intelligent and Robotic Systems*, 40(1):1–22, 2004.
38. Da Sun, Fazel Naghdy, and Haiping Du. Application of wave-variable control to bilateral teleoperation systems: A survey. *Annual Reviews in Control*, 38(1):12–31, 2014.
39. Romeo Ortega, Julio Antonio Lora Perez, Per Johan Nicklasson, and Hebertt Sira-Ramirez. *Passivity-Based Control of Euler-Lagrange Systems: Mechanical, Electrical and Electromechanical Applications*. Springer Science & Business Media, London, 2013.
40. Sukhan Lee and Hahk Sung Lee. Modeling, design, and evaluation of advanced teleoperator control systems with short time delay. *IEEE Transactions on Robotics and Automation*, 9(5):607–623, 1993.
41. G Hirzinger, J Heindl, and K Landzettel. Predictive and knowledge-based telerobotic control concepts. In *IEEE International Conference on Robotics and Automation*, pp. 1768–1777, IEEE, Scottsdale, AZ, USA May 1989.
42. Paolo Arcara and Claudio Melchiorri. Control schemes for teleoperation with time delay: A comparative study. *Robotics and Autonomous systems*, 38(1):49–64, 2002.

43. Saghir Munir and Wayne J Book. Internet-based teleoperation using wave variables with prediction. *IEEE/ASME Transactions on Mechatronics*, 7(2):124–133, 2002.
44. Andrew C Smith and Keyvan Hashtrudi-Zaad. Smith predictor type control architectures for time delayed teleoperation. *The International Journal of Robotics Research*, 25(8):797–818, 2006.
45. José Maria Azorn, O Reinoso, Rafael Aracil, and Manuel Ferre. Generalized control method by state convergence for teleoperation systems with time delay. *Automatica*, 40(9):1575–1582, 2004.
46. Dai Hanawa and Tatsuhiro Yonekura. A proposal of dead reckoning protocol in distributed virtual environment based on the taylor expansion. In *2006 International Conference on Cyberworlds*, pp. 107–114, Lausanne, Switzerland, IEEE, November 2006.
47. Luis F Penin and Kotaro Matsumoto. Teleoperation with time delay: A survey and its use in space robotics. Technical report, National Aerospace Laboratory (NAL) Japan, 2002.
48. Thomas B Sheridan. Space teleoperation through time delay: review and prognosis. *IEEE Transactions on Robotics and Automation*, 9(5):592–606, 1993.
49. Won S Kim, Blake Hannaford, and AK Fejczy. Force-reflection and shared compliant control in operating telemanipulators with time delay. *IEEE Transactions on Robotics and Automation*, 8(2):176–185, 1992.
50. Blake Hannaford, Laurie Wood, Douglas A McAffee, and Haya Zak. Performance evaluation of a six-axis generalized force-reflecting teleoperator. *IEEE Transactions on Systems, Man, and Cybernetics*, 21(3):620–633, 1991.
51. Gregory Tholey, Jaydev P Desai, and Andres E Castellanos. Force feedback plays a significant role in minimally invasive surgery: results and analysis. *Annals of surgery*, 241(1):102–109, 2005.
52. Maria V Ottermo, Marit Øvstedal, Thomas Langø, Øyvind Stavdahl, Yunus Yavuz, Tor A Johansen, and Ronald Mårvik. The role of tactile feedback in laparoscopic surgery. *Surgical Laparoscopy Endoscopy & Percutaneous Techniques*, 16(6):390–400, 2006.
53. Mohsin I Tiwana, Stephen J Redmond, and Nigel H Lovell. A review of tactile sensing technologies with applications in biomedical engineering. *Sensors and Actuators A: Physical*, 179:17–31, 2012.
54. Carol E Reiley, Takintope Akinbiyi, Darius Burschka, David C Chang, Allison M Okamura, and David D Yuh. Effects of visual force feedback on robot-assisted surgical task performance. *The Journal of thoracic and cardiovascular surgery*, 135(1):196–202, 2008.
55. Árpád Takács, Imre J Rudas, and Tamás Haidegger. Surface deformation and reaction force estimation of liver tissue based on a novel nonlinear mass–spring–damper viscoelastic model. *Medical & Biological Engineering & Computing*, 54(10):1553–1562, 2016.
56. Allison M Okamura, Lawton N Verner, CE Reiley, and Mohsen Mahvash. Haptics for robot-assisted minimally invasive surgery. In Kaneko M, and Nakamura Y. (eds.) *Robotics Research. Springer Tracts in Advanced Robotics, vol 66.*, pp. 361–372, Springer, Berlin, Heidelberg2010.
57. Dan Morris, Hong Tan, Federico Barbagli, Timothy Chang, and Kenneth Salisbury. Haptic feedback enhances force skill learning. In *Second Joint EuroHaptics Conference and Symposium on Haptic Interfaces for Virtual Environment and Teleoperator Systems (WHC'07)*, pp. 21–26, Washington, DC, USA, IEEE, March 2007.
58. Kevin Montgomery, Cynthia Bruyns, Joel Brown, Stephen Sorkin, Frederic Mazzella, Guillaume Thonier, Arnaud Tellier, Benjamin Lerman, and Anil Menon. Spring: A general framework for collaborative, real-time surgical simulation. *Studies in Health Technology and Informatics*, pp. 296–303, IOS Press, Amsterdam, 2002.
59. Yonghang Tai, Lei Wei, Hailing Zhou, Saeid Nahavandi, and Junsheng Shi. Tissue and force modelling on multi-layered needle puncture for percutaneous surgery training. In *Proceddings of the 2015 IEEE International Conference on Systems, Man, and Cybernetics*, pp. 2923–2927, Budapest, IEEE, October 2016.

60. Iman Brouwer, Jeffrey Ustin, L Bentiey, A Dhruv, and F Tendick. Measuring in vivo animal soft tissue properties for haptic modeling in surgical. *Medicine Meets Virtual Reality (MMVR)*, 81:69, 2001.
61. Herve Delingette. Toward realistic soft-tissue modeling in medical simulation. *Proceedings of the IEEE*, 86(3):512–523, 1998.
62. Mahdi Tavakoli, Arash Aziminejad, Rajni V Patel, and Mehrdad Moallem. High-fidelity bilateral teleoperation systems and the effect of multimodal haptics. *IEEE Transactions on Systems, Man, and Cybernetics, Part B (Cybernetics)*, 37(6):1512–1528, 2007.
63. Árpád Takács, Levente Kovács, Imre J Rudas, Radu-Emil Precup, and Tamás Haidegger. Models for force control in telesurgical robot systems. *Acta Polytechnica Hungarica*, 12(8):95–114, 2015.
64. Evren Samur, Mert Sedef, Cagatay Basdogan, Levent Avtan, and Oktay Duzgun. A robotic indenter for minimally invasive measurement and characterization of soft tissue response. *Medical Image Analysis*, 11(4):361–373, 2007.
65. Marco Beccani, Christian Di Natali, Levin J Sliker, Jonathan A Schoen, Mark E Rentschler, and Pietro Valdastri. Wireless tissue palpation for intraoperative detection of lumps in the soft tissue. *IEEE Transactions on Biomedical Engineering*, 61(2):353–361, 2014.
66. Guillaume Picinbono, Herve Delingette, and Nicholas Ayache. Nonlinear and anisotropic elastic soft tissue models for medical simulation. In *Robotics and Automation, 2001. Proceedings 2001 ICRA. IEEE International Conference on*, volume 2, pp. 1370–1375, Seoul, South Korea, IEEE, May 2001.
67. Ana Luisa Trejos, Jagadeesan Jayender, MP Perri, Michael D Naish, Rajnikant V Patel, and RA Malthaner. Robot-assisted tactile sensing for minimally invasive tumor localization. *The International Journal of Robotics Research*, 28(9):1118–1133, 2009.
68. Christopher R Wagner and Robert D Howe. Force feedback benefit depends on experience in multiple degree of freedom robotic surgery task. *IEEE Transactions on Robotics*, 23(6):1235–1240, 2007.
69. Tim Horeman, Sharon P Rodrigues, John J van den Dobbelsteen, Frank-Willem Jansen, and Jenny Dankelman. Visual force feedback in laparoscopic training. *Surgical Endoscopy*, 26(1):242–248, 2012.
70. Greig L McCreery, Ana Luisa Trejos, Michael D Naish, Rajni V Patel, and Richard A Malthaner. Feasibility of locating tumours in lung via kinaesthetic feedback. *The International Journal of Medical Robotics and Computer Assisted Surgery*, 4(1):58–68, 2008.
71. KJ Parker. A microchannel flow model for soft tissue elasticity. *Physics in Medicine and Biology*, 59(15):4443–4457, 2014.
72. Walter Maurel, Yin Wu, Daniel Thalmann, and Nadia Magnenat Thalmann. *Biomechanical Models for Soft Tissue Simulation*. Springer, Berlin, Heidelberg,1998.
73. Jacob Rosen, Jeffrey D Brown, Smita De, Mika Sinanan, and Blake Hannaford. Biomechanical properties of abdominal organs in vivo and postmortem under compression loads. *Journal of Biomechanical Engineering*, 130(2):210201–210217, 2008.
74. Nadia Alkhouli, Jessica Mansfield, Ellen Green, James Bell, Beatrice Knight, Neil Liversedge, Ji Chung Tham, Richard Welbourn, Angela C Shore, Katarina Kos, et al. The mechanical properties of human adipose tissues and their relationships to the structure and composition of the extracellular matrix. *American Journal of Physiology-Endocrinology and Metabolism*, 305(12):E1427–E1435, 2013.
75. Kevin L Troyer, Snehal S Shetye, and Christian M Puttlitz. Experimental characterization and finite element implementation of soft tissue nonlinear viscoelasticity. *Journal of Biomechanical Engineering*, 134(11):114501–114508, 2012.
76. Csaba Urbán, Peter Galambos, Gyorgy Györök and Tamas Haidegger Simulated medical ultrasound trainers a review of solutions and applications. *Acta Polytechnica Hungarica*, 15(7): 111–131, 2018.

77. Min Li, Jelizaveta Konstantinova, Emanuele L Secco, Allen Jiang, Hongbin Liu, Thrishantha Nanayakkara, Lakmal D Seneviratne, Prokar Dasgupta, Kaspar Althoefer, and Helge A Wurdemann. Using visual cues to enhance haptic feedback for palpation on virtual model of soft tissue. *Medical & Biological Engineering & Computing*, 53(11):1177–1186, 2015.
78. Florence Ching Leong. *Modelling and Analysis of a new Integrated Radiofrequency Ablation and Division Device*. PhD Dissertation, National University of Singapore, Singapore, 2009.
79. Zhongkui Wang and Shinichi Hirai. Modeling and parameter estimation of rheological objects for simultaneous reproduction of force and deformation. In *International Conference on Applied Bionics and Biomechanics,* Venice, Italy, October 2010.
80. A Constantinesco, H Schwerdt, and J Chambron. Testing device to determine the dynamic rheological properties of soft tissues in biaxial elongation. *Medical and Biological Engineering and Computing*, 19(2):129–134, 1981.
81. Xin Wang, Jonathan A Schoen, and Mark E Rentschler. A quantitative comparison of soft tissue compressive viscoelastic model accuracy. *Journal of the Mechanical Behavior of Biomedical Materials*, 20:126–136, 2013.
82. C Machiraju, A-V Phan, AW Pearsall, and S Madanagopal. Viscoelastic studies of human subscapularis tendon: relaxation test and a wiechert model. *Computer Methods and Programs in Biomedicine*, 83(1):29–33, 2006.
83. Árápad Takács, József K Tar, Tamás Haidegger, and Imre J Rudas. Applicability of the maxwell-kelvin model in soft tissue parameter estimation. In *2014 IEEE 12th International Symposium on Intelligent Systems and Informatics (SISY)*, pp. 115–119, IEEE, Subotica, Serbia September 2014.
84. Arpad Takacs, Péter Galambos, Péter Pausits, Imre J Rudas, and Tamás Haidegger. Nonlinear soft tissue models and force control for medical cyber-physical systems. In *2015 IEEE International Conference on Systems, Man, and Cybernetics (SMC)*, pp. 1520–1525, Hong Kong, ChinaIEEE, September 2015.
85. Árpád Takács, József Kuti, Tamás Haidegger, Péter Galambos, and Imre Rudas. Polytopic model based interaction control for soft tissue manipulation. In *2016 IEEE International Conference on Systems, Man, and Cybernetics*. IEEE, Budapest, Hungary October 2016.
86. P Baranyi, Y Yam, and P Varlaki. Tensor Product model transformatoin in polytopic model-based control. *Automation and Control Engineering.* CRC Press, Boca Raton, FL, 2017.
87. Árpád Takács, Tamás Haidegger, Jozsef Galambos, Peter, and Imre J Kuti Rudas. Nonlinear soft tissue mechanics based on polytopic tensor product modeling. In *2016 IEEE 14th International Symposium on Applied Machine Intelligence and Informatics (SAMI)*, pp. 211–215, IEEE, Herl'any, Slovakia January 2016.
88. Lőrinc Márton, Zoltán Szántó, Tamás Haidegger, Péter Galambos, and József Kövecses. Internet-based Bilateral Teleoperation using a revised time-domain passivity controller. *Acta Polytechnica Hungarica* 14 (8): 27–45, 2017.